References

A., C., Gringarten, A., Al-Lamki, S., Daungkaew. Well Test Analysis in Gas-Condensate Reservoirs., paper SPE 62920. presented at the 2000 SPE Annual Technical Conference and Exhibition, Dallas, Texas, U.S.A., 1-4 October 2000.

Amit K. Sarkar, Jaedong, Lee, and Ekrem Kasap. Adverse Effects of Poor Mudcake Quality : A Supercharging and Fluid Sampling Study., paper SPE 64227. presented at the SPE Annual Technical Conference and Exhibition, New Orleans, U.S.A., 27-30 September 1998.

Athichanagorn, S. Advanced Reservoir Engineering Lecture Note. Unpublished, September 2003.

Bourdet, D. Pressure Behavior of Layered Reservoir with Crossflow., paper SPE 13628, presented a the SPE 1985 California Regional Meeting, Bakerfield, California, U.S.A.; 27-29 March 1985.

Cinco, H., Samaniego, F. Transient Pressure Analysis: Finite Conductivity Fracture Case Versus Damaged Fracture Case., paper SPE 10179. presented at the 6th SPE Annual Technical Conference and Exhibition, San Antonio, Texas, U.S.A., 5-7 October 1981b.

Culham, W.W. Pressure Buildup Equations for Spherical Flow Regime Problems., paper SPE 4053. presented at the SPE-AIME 47th Annual Fall Meeting, San Antonio, Texas, U.S.A., 8-11 October 1974.

Daungkaew, S., Prosser, D.J., Manescu, A, and Molares, M. An Illustration of the Information that can be Obtained from Pressure Transient Analysis of Wireline Formation Test Data., paper SPE 88560. presented at the SPE Asia Pacific Oil and Gas Conference and Exhibition, Perth, Australia, 18-20 October 2004.

Dussan, E.B., and Sharma,Y. An Analysis of the Pressure Response of a Single Probe Formation tester., paper SPE 16801. presented at the 62nd Annual Fall Conference and Exhibition, Dallas, Texas, U.S.A., 27-30 September 1987.

Goode, P.A., Thambynayagam, R.K.M. Influence of an Invaded Zone on a Multiprobe Formation Tester., paper SPE 23030. presented at the SPE Asia Pacific Conference, Perth, Australia, 4-7 November 1991.

Goode, P.A., and Thambynayagam, R.K.M. Permeability Determination with a Multiprobe Formation Tester., paper SPE 20737. SPE Formation Evaluation December 1992.

Gok, I., M., M., Onur, P., S., Hegeman, F.J., Kuchuk. Effect of an Invaded Zone on Pressure Transient Data Form Multi-Probe and Packer-Probe Wireline Formation Testers in Single and Multilater Systems., paper SPE 84093. presented at the SPE Annual Technical Conference and Exhibition, Denver, Colorado, U.S.A., 5-8 October 2003.

Horne, D. R., Pressure Build-up in Wells, The Third World Petroleum Congress, 1951, The Hague, Holland, pp. 503-521.

Horne, R., N. Modern Well Test Analysis: A Computer-Aided Approach. Second Edition, Petroway, Inc., U.S.A., 1998.

Jianghui Wu, and Carlos Torres-Verdin. Inversion of Multi-Phase Petrophysical Properties Using Pumpout Sampling Data Acquired With a Wireline Formation Tester., paper SPE 77345. presented at the SPE Annual Technical Conference and Exhibition, San Antonio, Texas, U.S.A., 29 September – 2 October 2002.

Kuchuk, F.J., Ramakrishnan, T.S., and Dave, Y. Interpretation of Wireline Formation Tester Packer and Probe Pressures., paper SPE 28404. presented at the 69th Annual Technical Conference and Exhibition, New Orleans, Louisiana, U.S.A., 25-28 September 1994.

Kuchuk, F.J. A New Method for Determination of Reservoir Pressure., paper SPE 56418. presented at the 1999 SPE Annual Technical Conference and Exhibition, Houston, Texas, U.S.A., 3-6 October 1999.

Mark, A., Proett, Wilson, Chin, Jianghui, W., and Mohan, M. Sample Quality Prediction with Integrated Oil and Water-based Mud Invasion Modeling., paper SPE 77964. presented at the SPE Asia Pacific Oil and Gas Conference and Exhibition, Melbourne, Australia, 8-10 October 2002.

Mayank, Malik, Carlos Torres-Verdin, and Kamy, Sepehrnoori. Robust and Efficient Simulation of Formation-Tester Measurements with a Rigorous Compostional Simulation Code., paper SPE 102151. presented at the SPE Annual Technical Conference and Exhibition, San Antonio, Texas, U.S.A., 24-27 September 2006.

Moran, J.H., and Flinklea, E.E. Theoretical Analysis of Pressure Phenomena Associated with the Wireline Formation Test Data., paper SPE 177. presented at the 36th Annual Fall Meeting of SPE, Dallas, Nevada, U.S.A., 8-11 October 1962.

Palasarn, D. Evaluation of Reservoir Properties From Wireline Formation Test in Multilayer Reservoir. Master's thesis, Department of Mining and Petroleum Engineering, Faculty of Engineering, Chulalongkorn University, 2006.

R., R., Jackson, R., Banerjee, and R.K.M., Thambynayagam. An Integrated Approach to Interval Pressure Transient Test Analysis Using Analytical and Numerical Methods., paper SPE 81515. presented at the SPE 13th Middle East Oil Show & Conference, Bahrain, 5-8 April 2003.

Stewart, G., and Wittman, M. Interpretation of the Pressure Response of the Repeat Formation Tester., paper SPE 8362. presented at the 54th Annual Fall Conference and Exhibition, Las Vegas, Nevada, U.S.A., 23-26 September 1979.

Whittle, T.M., Lee, J., Gringarten, A. C. Will Wireline Formation Tests Replace Well Tests?, paper SPE 84086. presented at SPE Annual Technical Conference and Exhibition, Denver, Colorado, U.S.A., 5-8 October 2003.

Xian, C., Carnegie, C., Al Raisi, M. R., Petricola, M., Chen, J. An Integrated Efficient Approach To Perform IPTT Interpretation., paper SPE 88561. presented at the SPE Asia Pacific Oil and Gas Conference, Perth, Australia, 18-20 October 2004.

APPENDICES

APPENDIX A

Script example from ECLIPSE simulator:

Oil_Lg-K10_ggo.INC

```
GRIDUNIT
--
-- Grid data units
--
 'FEET' /
COORDSYS
--
-- Coordinate System Information
--
      1*        1* 'INCOMP' 'SEPARATE' /

INRAD
--
-- Inner Radius
--
    0.25 /
DRV
0.034033733 0.061731054 0.083138224 0.111969 0.150797747 0.203091575
0.273519921 0.368371495 0.496115814 0.668159466 0.899864626 1.211920786
1.632192164 2.198205767 2.960502263 3.987148873 5.369817256 7.231969078
9.739880196 13.11748781 17.66638634 23.79275749 32.04363915 43.15577169
58.12138319 78.27678783 105.4217084 141.979978 191.2159691 257.5260776
/

DTHETAV
7.802855753 10.30162849 11.83673805 13.6006038 15.62731413 17.95603713
20.63177759 23.70624674 27.2388616 31.29789331 31.29789331 27.2388616
```

23.70624674 20.63177759 17.95603713 15.62731413 13.6006038 11.83673805
10.30162849 7.802942552
/

--*BOX panel edit: TOPS set equal to 8100 ft for box (1:30, 1:20, 1:1)
--*BOX panel edit: TOPS set equal to 8101.905 ft for box (1:30, 1:20, 2:2)
--*BOX panel edit: TOPS set equal to 8103.464 ft for box (1:30, 1:20, 3:3)
--*BOX panel edit: TOPS set equal to 8104.739 ft for box (1:30, 1:20, 4:4)
--*BOX panel edit: TOPS set equal to 8105.783 ft for box (1:30, 1:20, 5:5)
--*BOX panel edit: TOPS set equal to 8106.636 ft for box (1:30, 1:20, 6:6)
--*BOX panel edit: TOPS set equal to 8107.335 ft for box (1:30, 1:20, 7:7)
--*BOX panel edit: TOPS set equal to 8107.906 ft for box (1:30, 1:20, 8:8)
--*BOX panel edit: TOPS set equal to 8108.374 ft for box (1:30, 1:20, 9:9)
--*BOX panel edit: TOPS set equal to 8108.756 ft for box (1:30, 1:20, 10:10)
--*BOX panel edit: TOPS set equal to 8109.069 ft for box (1:30, 1:20, 11:11)
--*BOX panel edit: TOPS set equal to 8109.326 ft for box (1:30, 1:20, 12:12)
--*BOX panel edit: TOPS set equal to 8109.535 ft for box (1:30, 1:20, 13:13)
--*BOX panel edit: TOPS set equal to 8109.707 ft for box (1:30, 1:20, 14:14)
--*BOX panel edit: TOPS set equal to 8109.847 ft for box (1:30, 1:20, 15:15)
--*BOX panel edit: TOPS set equal to 8109.962 ft for box (1:30, 1:20, 16:16)
--*BOX panel edit: TOPS set equal to 8110.038 ft for box (1:30, 1:20, 17:17)
--*BOX panel edit: TOPS set equal to 8110.153 ft for box (1:30, 1:20, 18:18)
--*BOX panel edit: TOPS set equal to 8110.293 ft for box (1:30, 1:20, 19:19)
--*BOX panel edit: TOPS set equal to 8110.465 ft for box (1:30, 1:20, 20:20)
--*BOX panel edit: TOPS set equal to 8110.674 ft for box (1:30, 1:20, 21:21)
--*BOX panel edit: TOPS set equal to 8110.931 ft for box (1:30, 1:20, 22:22)
--*BOX panel edit: TOPS set equal to 8111.244 ft for box (1:30, 1:20, 23:23)
--*BOX panel edit: TOPS set equal to 8111.626 ft for box (1:30, 1:20, 24:24)
--*BOX panel edit: TOPS set equal to 8112.094 ft for box (1:30, 1:20, 25:25)
--*BOX panel edit: TOPS set equal to 8112.665 ft for box (1:30, 1:20, 26:26)
--*BOX panel edit: TOPS set equal to 8113.364 ft for box (1:30, 1:20, 27:27)
--*BOX panel edit: TOPS set equal to 8114.217 ft for box (1:30, 1:20, 28:28)
--*BOX panel edit: TOPS set equal to 8115.261 ft for box (1:30, 1:20, 29:29)

--*BOX panel edit: TOPS set equal to 8116.536 ft for box (1:30, 1:20, 30:30)
--*BOX panel edit: TOPS set equal to 8118.095 ft for box (1:30, 1:20, 31:31)
--*BOX panel edit: TOPS added value 4940 ft for box (1:30, 1:20, 1:31)
--*BOX panel edit: TOPS added value -4940 ft for box (1:30, 1:20, 1:31)

--*BOX panel edit: DZ set equal to 1.905079 ft for box (1:30, 1:20, 1:1)
--*BOX panel edit: DZ set equal to 1.558705 ft for box (1:30, 1:20, 2:2)
--*BOX panel edit: DZ set equal to 1.275307 ft for box (1:30, 1:20, 3:3)
--*BOX panel edit: DZ set equal to 1.043436 ft for box (1:30, 1:20, 4:4)
--*BOX panel edit: DZ set equal to 0.8537226 ft for box (1:30, 1:20, 5:5)
--*BOX panel edit: DZ set equal to 0.6985022 ft for box (1:30, 1:20, 6:6)
--*BOX panel edit: DZ set equal to 0.5715032 ft for box (1:30, 1:20, 7:7)
--*BOX panel edit: DZ set equal to 0.4675948 ft for box (1:30, 1:20, 8:8)
--*BOX panel edit: DZ set equal to 0.3825785 ft for box (1:30, 1:20, 9:9)
--*BOX panel edit: DZ set equal to 0.3130196 ft for box (1:30, 1:20, 10:10)
--*BOX panel edit: DZ set equal to 0.2561076 ft for box (1:30, 1:20, 11:11)
--*BOX panel edit: DZ set equal to 0.2095431 ft for box (1:30, 1:20, 12:12)
--*BOX panel edit: DZ set equal to 0.1714448 ft for box (1:30, 1:20, 13:13)
--*BOX panel edit: DZ set equal to 0.1402734 ft for box (1:30, 1:20, 14:14)
--*BOX panel edit: DZ set equal to 0.1147695 ft for box (1:30, 1:20, 15:15)
--*BOX panel edit: DZ set equal to 0.07682954 ft for box (1:30, 1:20, 16:16)
--*BOX panel edit: DZ set equal to 0.1147695 ft for box (1:30, 1:20, 17:17)
--*BOX panel edit: DZ set equal to 0.1402734 ft for box (1:30, 1:20, 18:18)
--*BOX panel edit: DZ set equal to 0.1402734 ft for box (1:30, 1:20, 18:18)
--*BOX panel edit: DZ set equal to 0.1714448 ft for box (1:30, 1:20, 19:19)
--*BOX panel edit: DZ set equal to 0.2095431 ft for box (1:30, 1:20, 20:20)
--*BOX panel edit: DZ set equal to 0.2561076 ft for box (1:30, 1:20, 21:21)
--*BOX panel edit: DZ set equal to 0.3130196 ft for box (1:30, 1:20, 22:22)
--*BOX panel edit: DZ set equal to 0.3825785 ft for box (1:30, 1:20, 23:23)
--*BOX panel edit: DZ set equal to 0.4675948 ft for box (1:30, 1:20, 24:24)
--*BOX panel edit: DZ set equal to 0.5715032 ft for box (1:30, 1:20, 25:25)
--*BOX panel edit: DZ set equal to 0.6985022 ft for box (1:30, 1:20, 26:26)
--*BOX panel edit: DZ set equal to 0.8537226 ft for box (1:30, 1:20, 27:27)

--*BOX panel edit: DZ set equal to 1.043436 ft for box (1:30, 1:20, 28:28)

--*BOX panel edit: DZ set equal to 1.275307 ft for box (1:30, 1:20, 29:29)

--*BOX panel edit: DZ set equal to 1.558705 ft for box (1:30, 1:20, 30:30)

--*BOX panel edit: DZ set equal to 1.905079 ft for box (1:30, 1:20, 31:31)

Oil_Lg-K10_gpro.INC

--*BOX panel edit: ACTNUM set equal to 1 for box (1:20, 1:20, 1:31)

EQUALS

ACTNUM 1 /

/

--*BOX panel edit: PORO set equal to 0.18 for box (1:30, 1:20, 1:31)

EQUALS

PORO 0.18 /

/

--*BOX panel edit: PERMR set equal to 10 mD for box (1:30, 1:20, 1:31)

EQUALS

PERMR 10 /

/

--*BOX panel edit: PERMTHT set equal to 10 mD for box (1:30, 1:20, 1:31)

EQUALS

PERMTHT 10 /

/

--*BOX panel edit: PERMZ set equal to 1 mD for box (1:30, 1:20, 1:31)

EQUALS

PERMZ 1 /

/

Oil_Lg-K10_pvt.INC

DENSITY

```
--
-- Fluid Densities at Surface Conditions
--
    51.457   63.029   0.0437
/

PVDO
--
-- Dead Oil PVT Properties (No Dissolved Gas)
--
    1847.9   1.3129  0.34932
    2005.6   1.3088  0.35453
    2163.2   1.3053  0.36022
    2320.8   1.3023  0.36636
    2478.4   1.2997  0.37293
      2636   1.2974  0.37992
    2793.6   1.2954   0.3873
    2951.2   1.2935  0.39507
    3108.8   1.2919  0.40319
    3266.4   1.2904  0.41167
      3424   1.2891  0.42049
    3581.6   1.2879  0.42964
    3739.2   1.2868  0.43911
    3896.8   1.2857  0.44888
    4054.4   1.2848  0.45896
      4212   1.2839  0.46932
    4369.6   1.2831  0.47996
    4527.2   1.2824  0.49088
    4684.8   1.2816  0.50206
      5000   1.2804  0.52515
/

RSCONSTT
```

```
--
-- Constant Rs per PVT Region
--
   0.58721    1847.9
/

PVTW
--
-- Water PVT Properties
--
      3450    1.0235 2.9111e-006  0.30286       1*
/

ECHO
ROCK
--
-- Rock Properties
--
      5000 1.048e-006
/
```

Oil_Lg-K10_scal.INC

```
SWOF
--
-- Water/Oil Saturation Functions
--
     0.16283          0          1      15947
      0.2069 3.5397e-013    0.89751     5832.4
     0.25096 3.0203e-010    0.80055      564.75
     0.29502 1.5654e-008    0.70914      144.11
     0.33908 2.5771e-007    0.62327      54.684
     0.38314 2.2632e-006    0.54292      25.788
      0.4272 1.3357e-005    0.46808      13.954
```

0.47126 5.9918e-005 0.39872 8.3024
0.51532 0.0002199 0.33476 5.295
0.55939 0.00069228 0.27615 3.5609
0.60345 0.0019311 0.22281 2.4971
0.64751 0.0048848 0.1747 1.8113
0.69157 0.011397 0.13186 1.3512
0.73563 0.024846 0.094431 1.0319
0.77969 0.051126 0.062731 0.80391
0.82375 0.10009 0.037204 0.6372
0.86782 0.18763 0.018335 0.5127
0.91188 0.33858 0.0063942 0.418
0.95594 0.59069 0.00094699 0.3448
1 1 0 0.28739

/

0.30427 0 1 97263
0.34088 6.9503e-014 0.89751 35007
0.3775 8.6999e-011 0.80055 2798.6
0.41412 5.6421e-009 0.70914 638.44
0.45074 1.089e-007 0.62327 223.74
0.48735 1.0819e-006 0.54293 99.201
0.52397 7.0623e-006 0.46811 51.04
0.56059 3.4499e-005 0.39879 29.1
0.59721 0.00013631 0.33492 17.887
0.63382 0.00045801 0.27644 11.644
0.67044 0.0013543 0.22328 7.9306
0.70706 0.003611 0.17538 5.6032
0.74368 0.00884 0.13273 4.0804
0.78029 0.020144 0.095433 3.0479
0.81691 0.043183 0.063744 2.3264
0.85353 0.087827 0.038076 1.8092
0.89015 0.17062 0.018933 1.4299
0.92676 0.31839 0.0066738 1.1464

```
    0.96338     0.5733  0.0010007    0.93084
       1         1         0    0.76435
/

    0.47559          0          1  393270000
    0.50319 6.7502e-030    0.89751  319600000
    0.53079 4.9699e-023    0.80055  245930000
    0.55839 5.1678e-019    0.70914  172260000
    0.58599 3.6592e-016    0.62327   98585000
    0.61359  5.944e-014    0.54294   24914000
    0.64119 3.8049e-012    0.46814    4093400
    0.66879 1.2809e-010    0.39889     889040
    0.69639 2.6941e-009    0.33518     236840
    0.72399 3.9564e-008    0.27701      73747
    0.75159 4.3763e-007    0.22438      25970
     0.7792  3.849e-006    0.17728      10103
     0.8068 2.8014e-005    0.13573     4266.9
     0.8344 0.00017393   0.099687     1930.9
      0.862 0.00094309   0.069133     926.72
     0.8896  0.0045506   0.043998     467.88
     0.9172   0.019836   0.024234     246.88
     0.9448    0.07908  0.0099861     135.42
     0.9724     0.2913  0.0018711     76.873
       1         1         0    44.996
/
```

Oil_Lg-K10_init.INC

```
EQUIL
--
-- Equilibration Data Specification
--
  8110   5000   8200    1*    1*    1*    1*    1*    1*    1*    1*
/
```

Oil_Lg-K10_sch.INC

```
WELSPECS
'WELL1' '1' 1 1 8120 'OIL' 1* 'STD' 'SHUT' 'YES' 1* 'SEG' 3* 'STD' /
/

RPTRST
'BASIC=6' 'NORST=0' /


TUNING
2e-006 0.0001 2e-006 7* /
11* /
10* /

COMPDAT
'WELL1' 1 1 16 16 'OPEN' 2* 0.5 3* 'Z' 1* /
/

SKIP
WBOREVOL
'WELL1' 0.5 1* /
/

ENDSKIP
WCONPROD
'WELL1' 'OPEN' 'ORAT' 0.8 4* 1847.9 3* /
/

DRSDT
10000 'ALL' /

TSTEP
0.02083 /
```

```
WELSPECS
'WELL1' '1' 1 1 8120 'OIL' 1* 'STD' 'SHUT' 'YES' 1* 'SEG' 3* 'STD' /
/

COMPDAT
'WELL1' 1 1 16 16 'OPEN' 2* 0.5 3* 'Z' 1* /
/

SKIP
WBOREVOL
'WELL1' 0.5 1* /
/

ENDSKIP
WCONPROD
'WELL1' 'OPEN' 'ORAT' 0 4* 1847.9 3* /
/

TUNING
2e-006 0.0001 2e-006 7* /
11* /
10* /

TSTEP
0.0625 /

END
```

Oil_Lg-K10_sum.INC

```
ALL
BPR
1 1 16 /
```

APPENDIX B

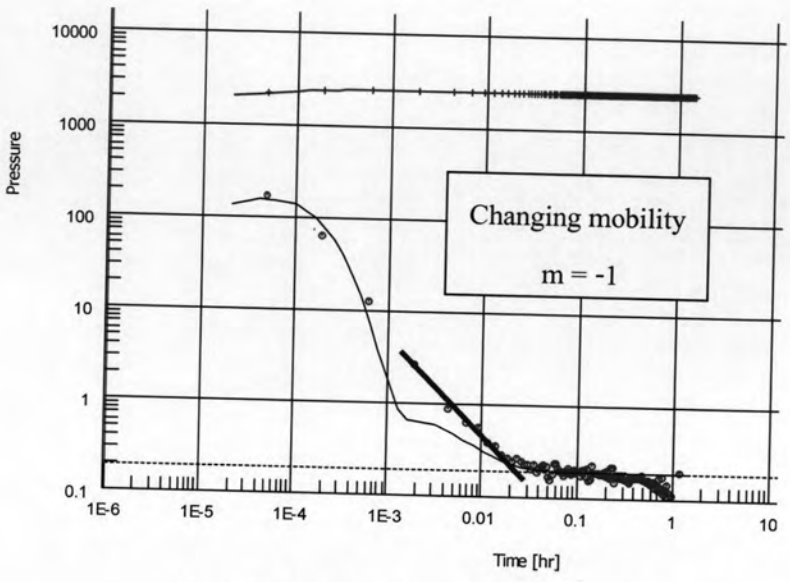

(a) Mobility ratio = 0.3

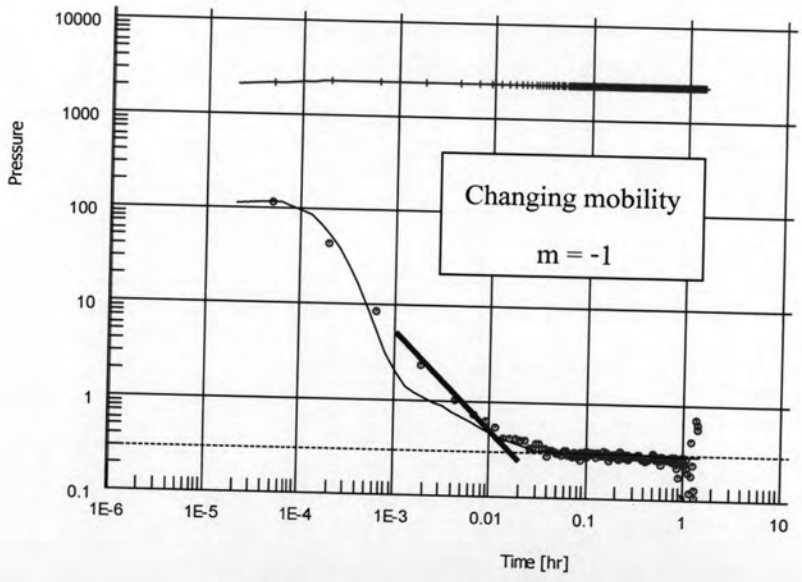

(b) Mobility ratio = 0.5

Figure B1 : Regression plots for different mobility ratios between invaded zone and uninvaded reservoir for case I.

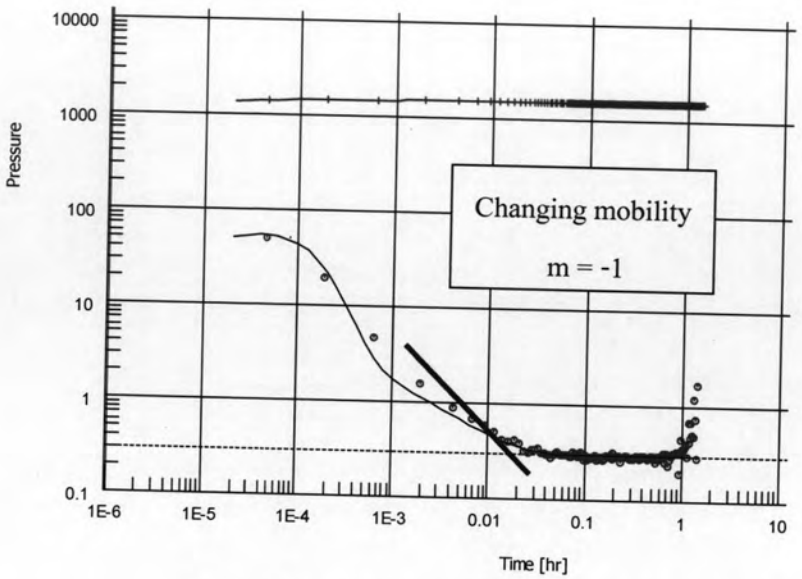

(c) Mobility ratio = 0.8

Figure B1 : Regression plots for different mobility ratios between invaded zone and uninvaded reservoir for case I (continued).

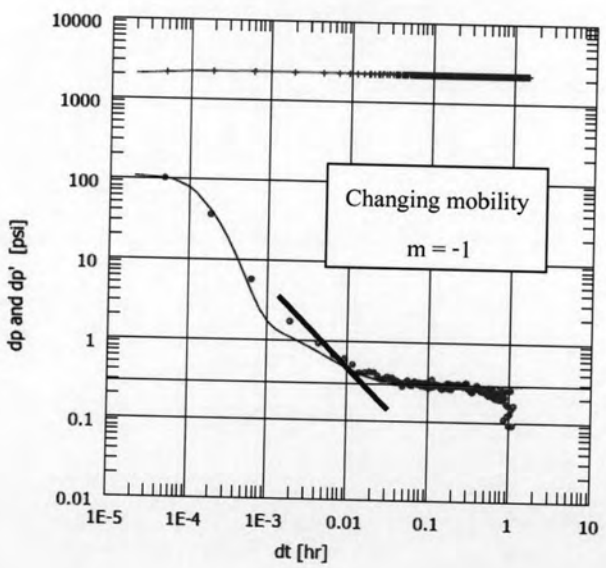

(a) Radius of Invasion = 0.44 ft.

Figure B2 : Regression plots for different radii of invasion for case I.

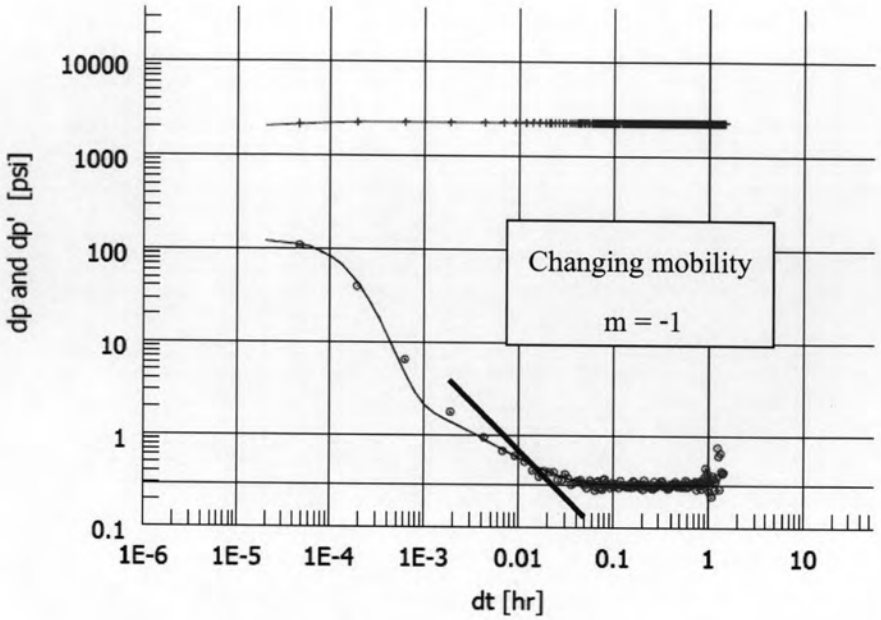

(b) Radius of Invasion = 0.64 ft.

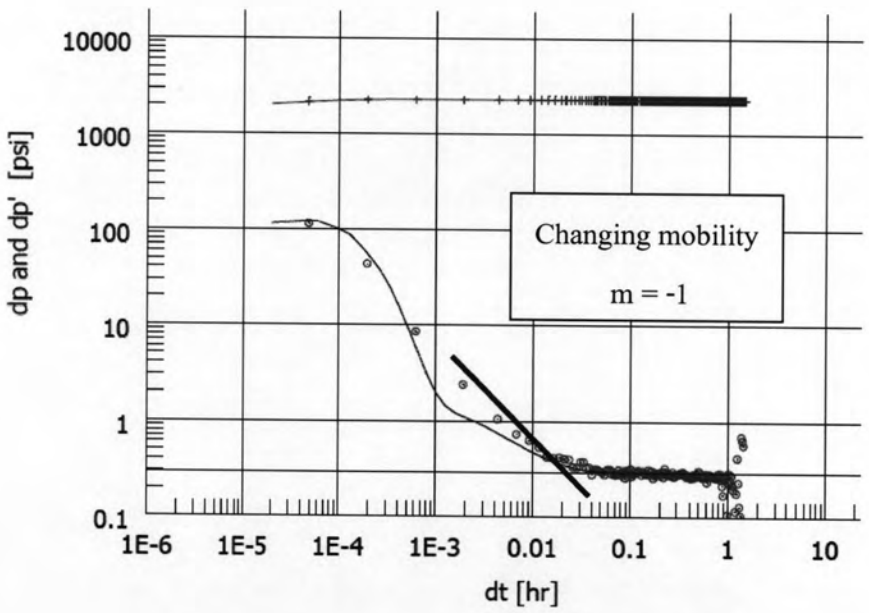

(c) Radius of Invasion = 1.28 ft.

Figure B2 : Regression plots for different radii of invasion for case I (continued).

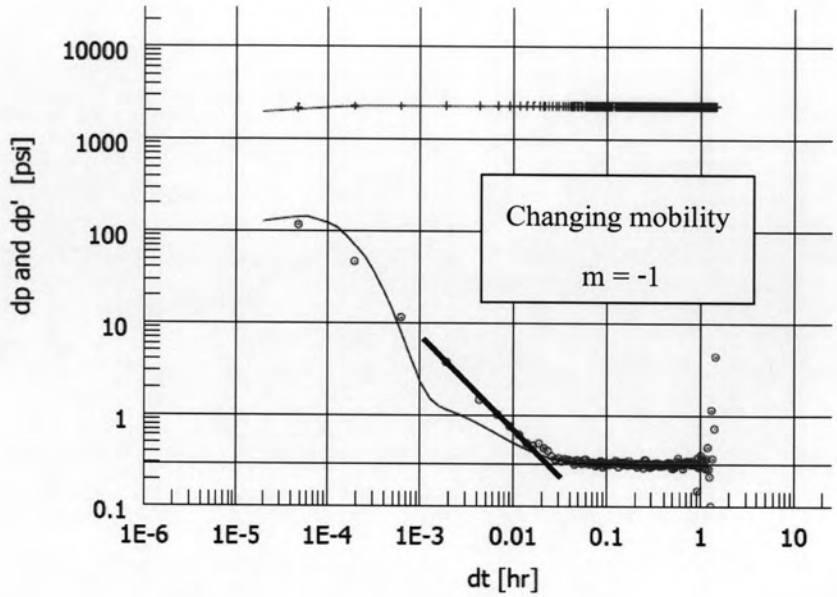

(d) Radius of Invasion = 3.35 ft.

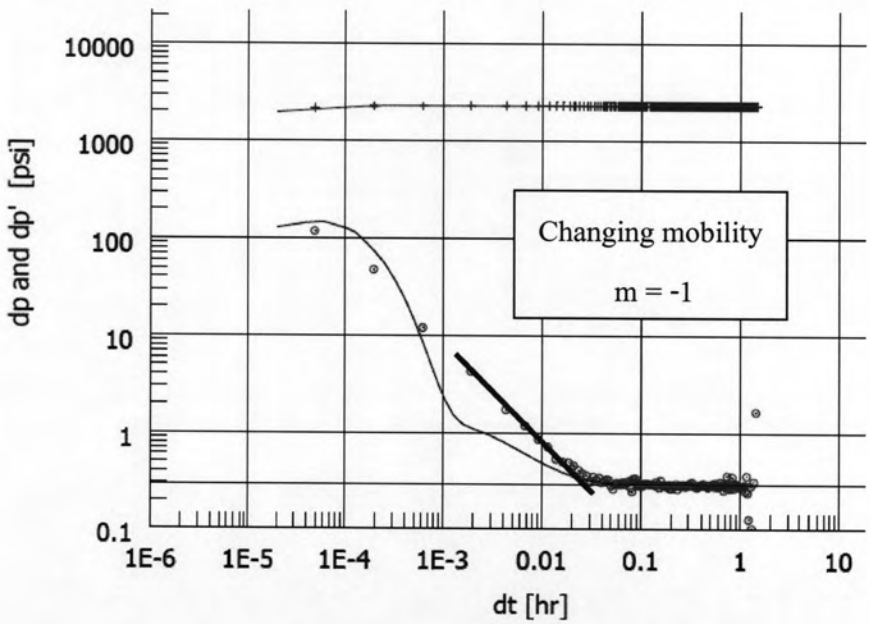

(e) Radius of Invasion = 4.56 ft.

Figure B2 : Regression plots for different radii of invasion for case I (continued).

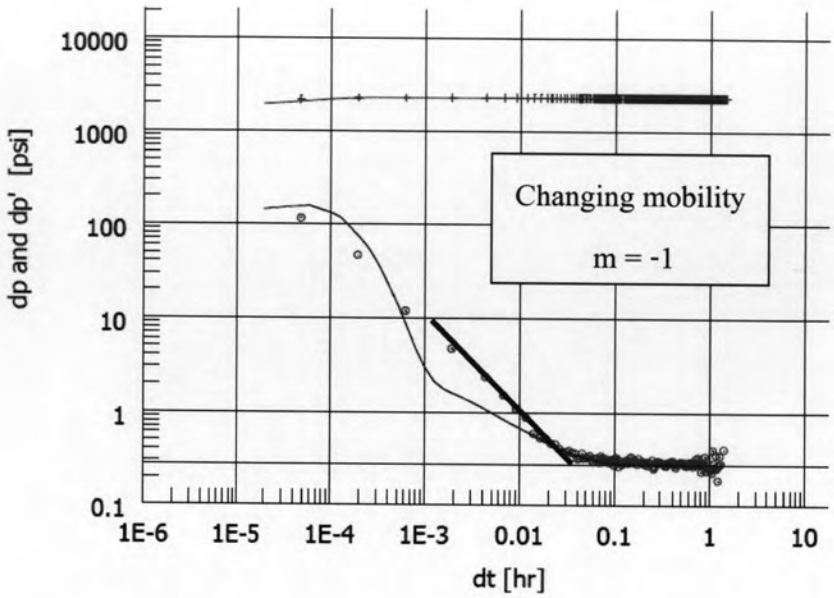

(f) Radius of Invasion = 6.19 ft.

Figure B2 : Regression plots for different radii of invasion for case I (continued).

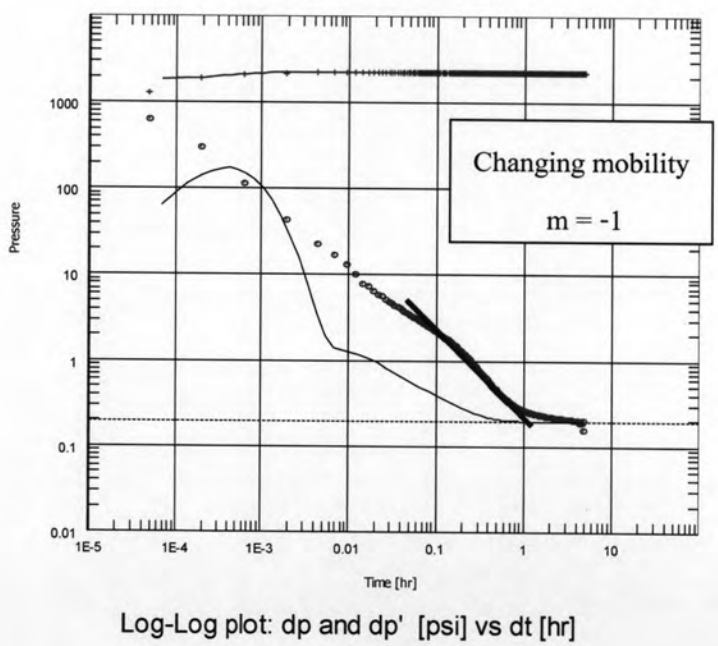

(a) Mobility ratio = 0.333

Figure B3 : Regression plots for different mobility ratios between invaded zone and uninvaded reservoir for case II.

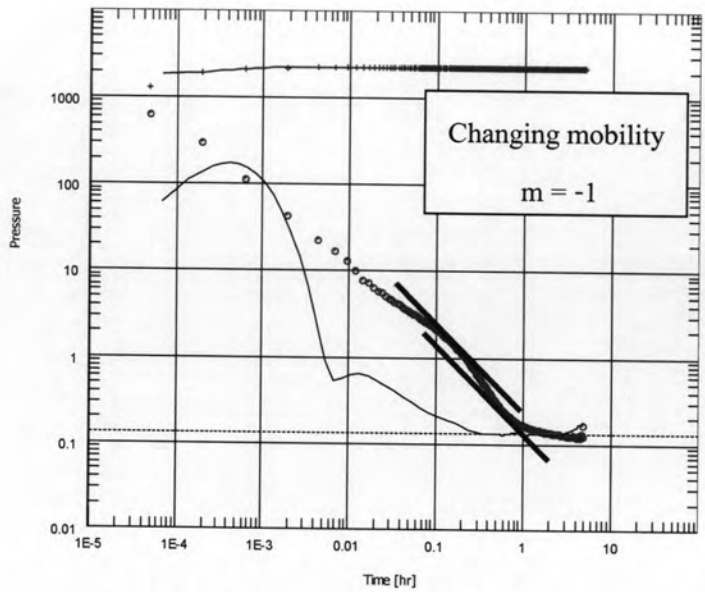

Log-Log plot: dp and dp' [psi] vs dt [hr]

(b) Mobility ratio = 0.2

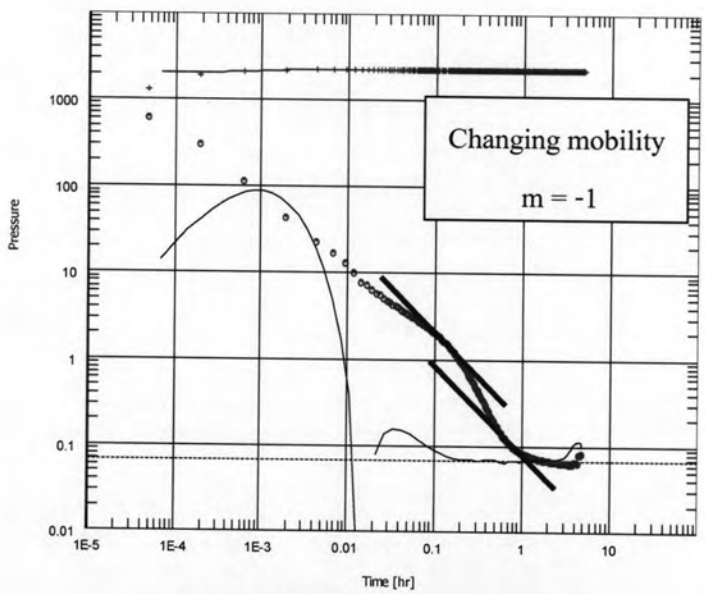

Log-Log plot: dp and dp' [psi] vs dt [hr]

(c) Mobility ratio = 0.1

Figure B3 : Regression plots for different mobility ratios between invaded zone and uninvaded reservoir for case II (continued).

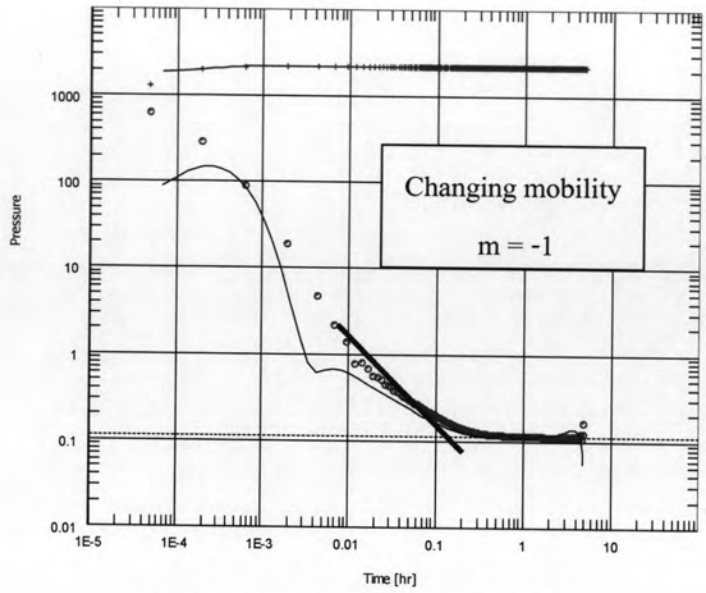

Log-Log plot: dp and dp' [psi] vs dt [hr]

(a) Radius of Invasion = 0.44 ft.

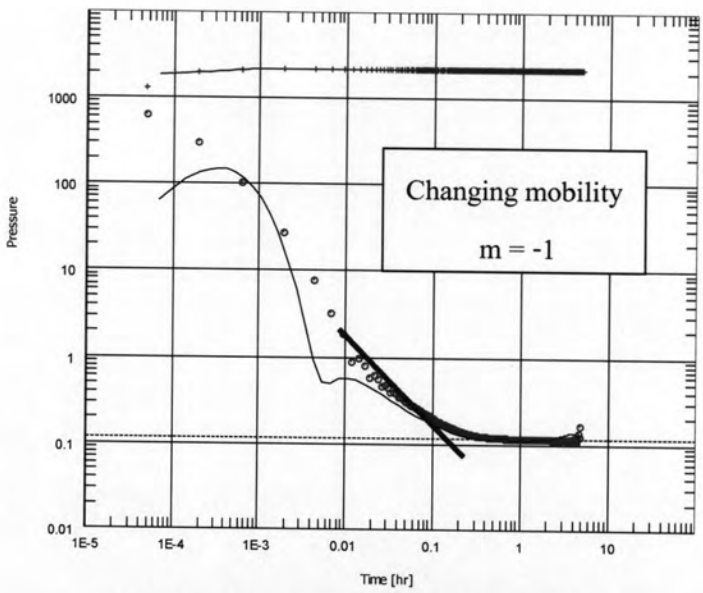

Log-Log plot: dp and dp' [psi] vs dt [hr]

(b) Radius of Invasion = 0.64 ft.

Figure B4 : Regression plots for different radii of invasion for case II.

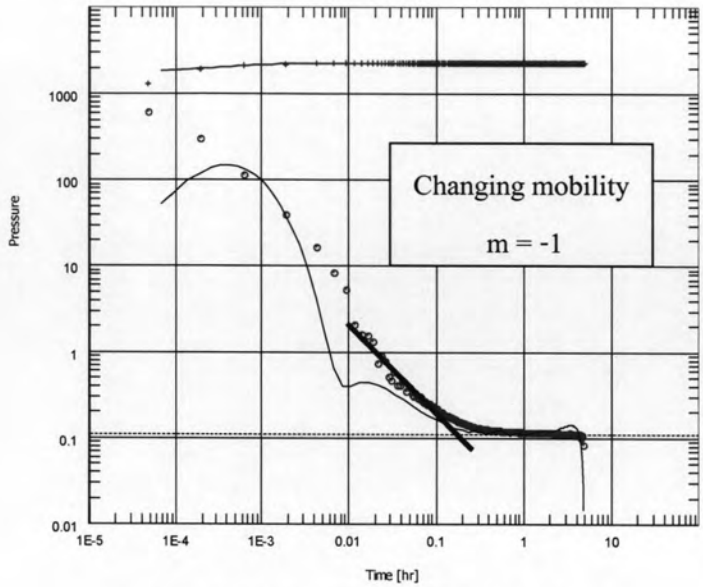

Log-Log plot: dp and dp' [psi] vs dt [hr]

(c) Radius of Invasion = 1.28 ft.

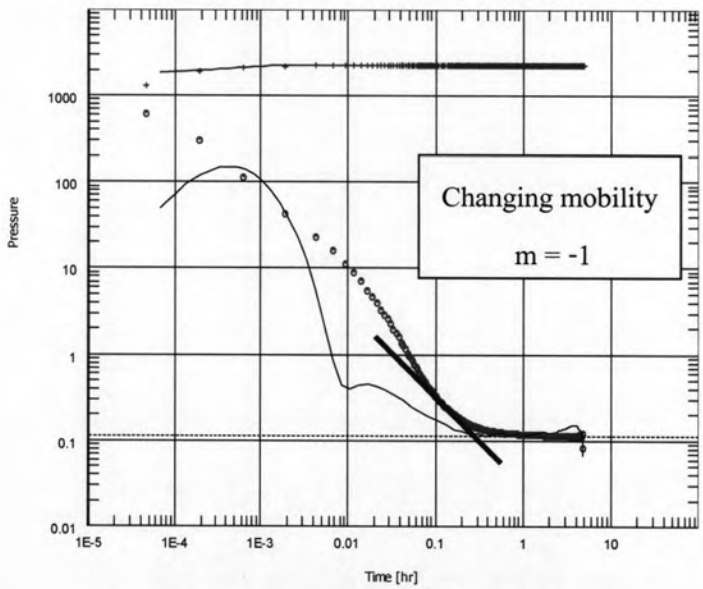

Log-Log plot: dp and dp' [psi] vs dt [hr]

(d) Radius of Invasion = 3.35 ft.

Figure B4 : Regression plots for different radii of invasion for case II (continued).

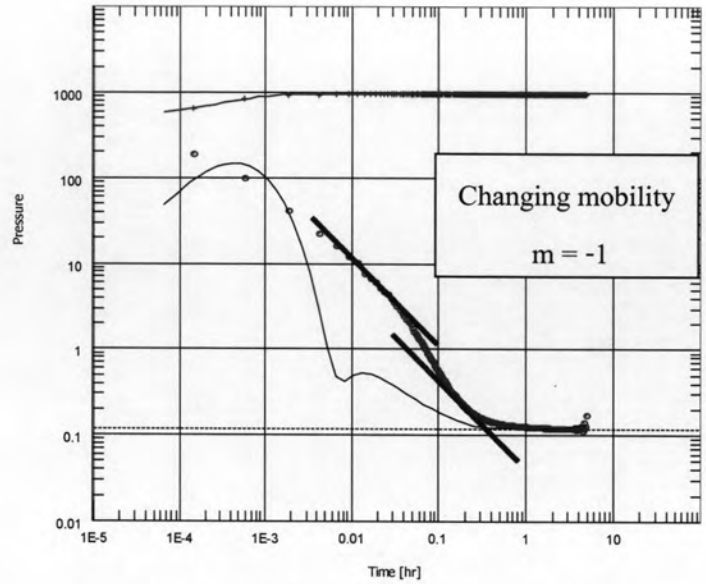

Log-Log plot: dp and dp' [psi] vs dt [hr]

(e) Radius of Invasion = 4.56 ft.

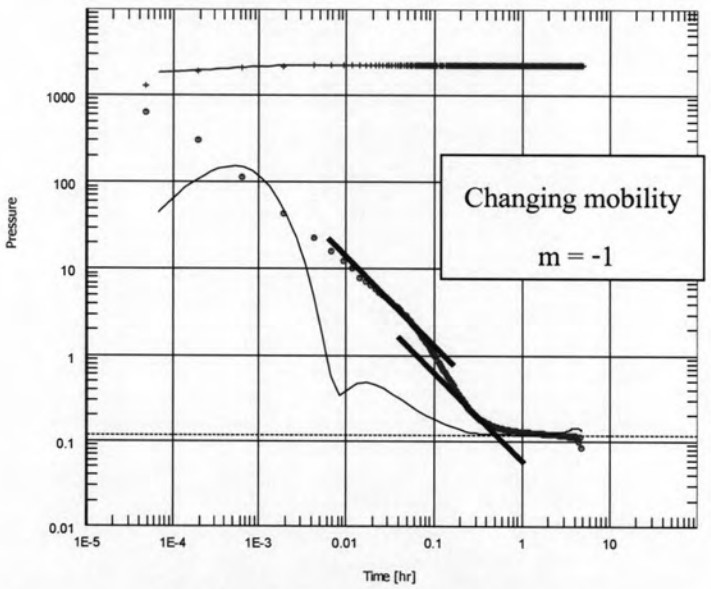

Log-Log plot: dp and dp' [psi] vs dt [hr]

(f) Radius of Invasion = 6.19 ft.

Figure B4 : Regression plots for different radii of invasion for case II (continued).

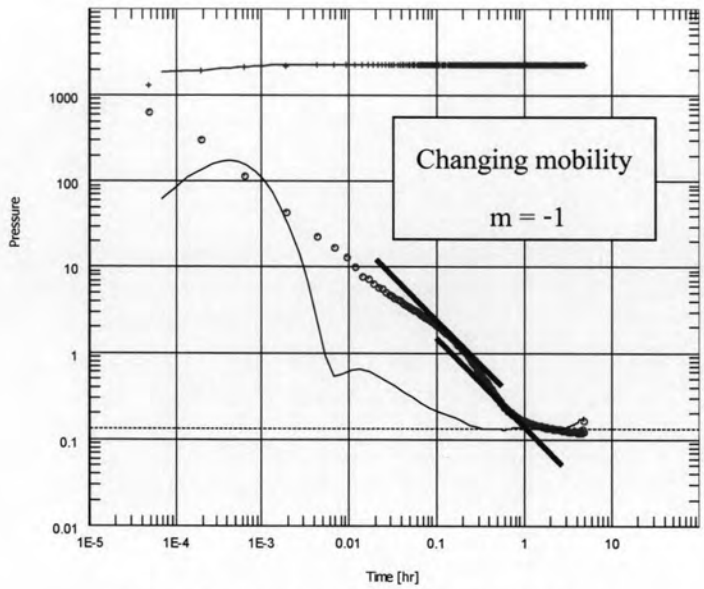

(g) Radius of Invasion = 11.35 ft.

Figure B4 : Regression plots for different radii of invasion for case II (continued).

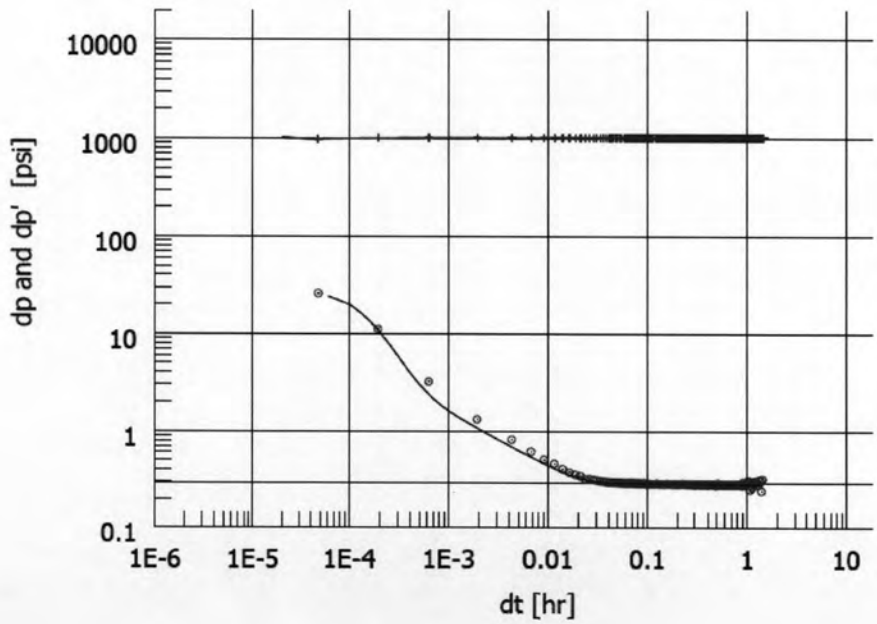

(a) Mobility ratio = 1.2

Figure B5 : Regression plots for different mobility ratios between stimulated zone and native reservoir for case I.

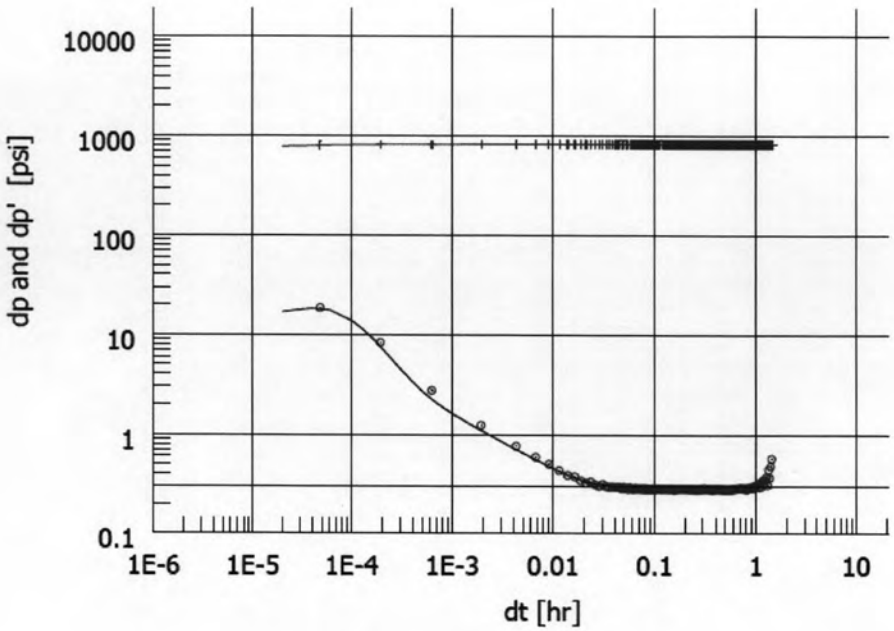

(b) Mobility ratio = 1.5

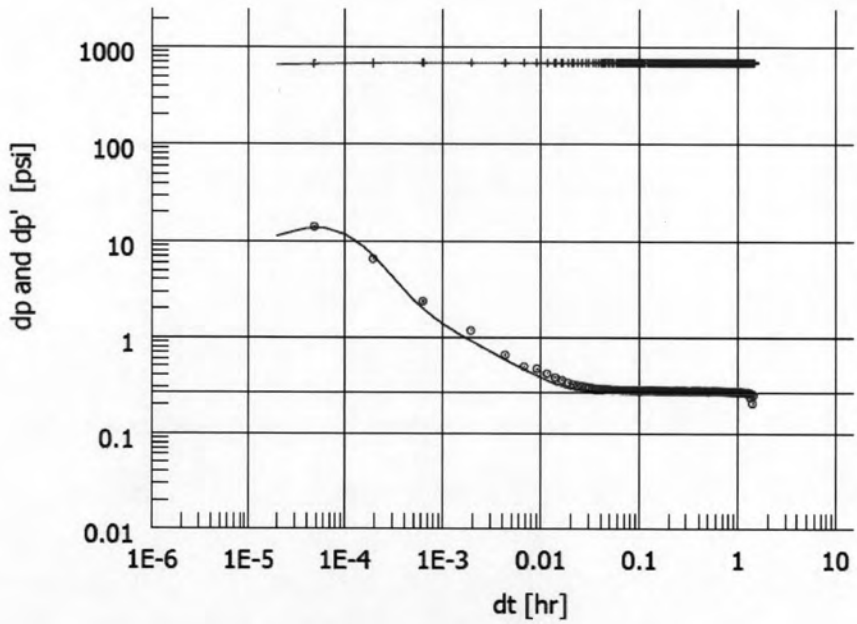

(c) Mobility ratio = 1.8

Figure B5 : Regression plots for different mobility ratios between stimulated zone and native reservoir for case I (continued).

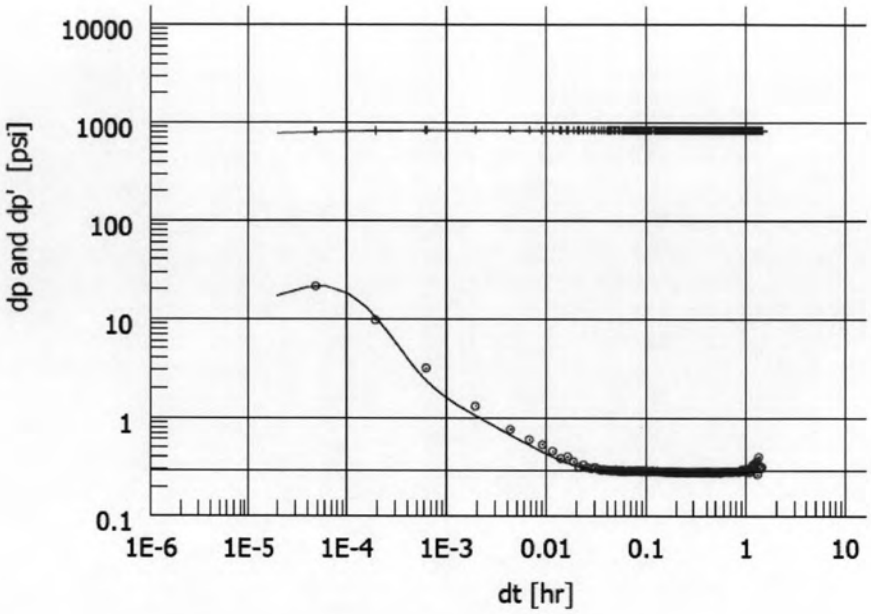

(a) Radius of stimulated zone = 0.44 ft.

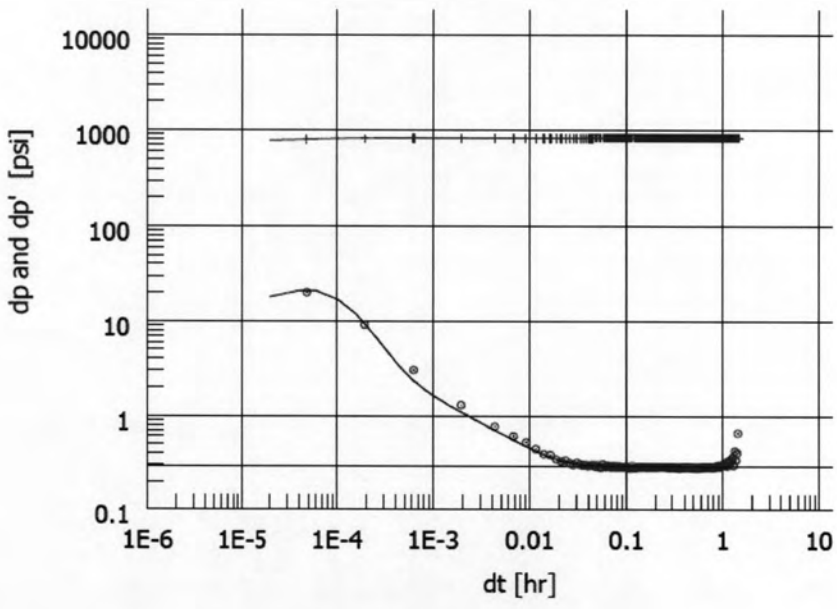

(b) Radius of stimulated zone = 0.64 ft.

Figure B6 : Regression plots for different radii of stimulated zone for case I.

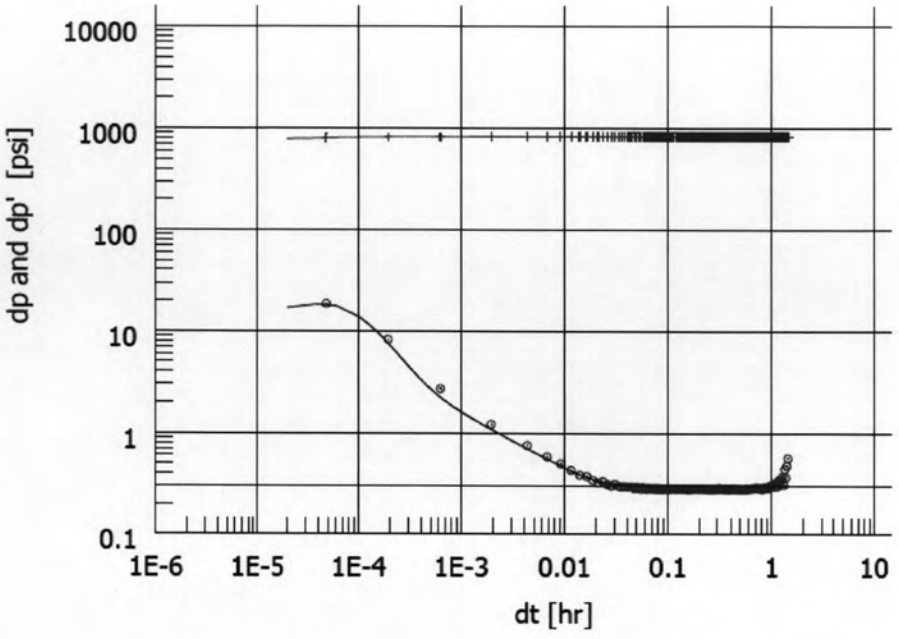

(c) Radius of stimulated zone = 1.28 ft.

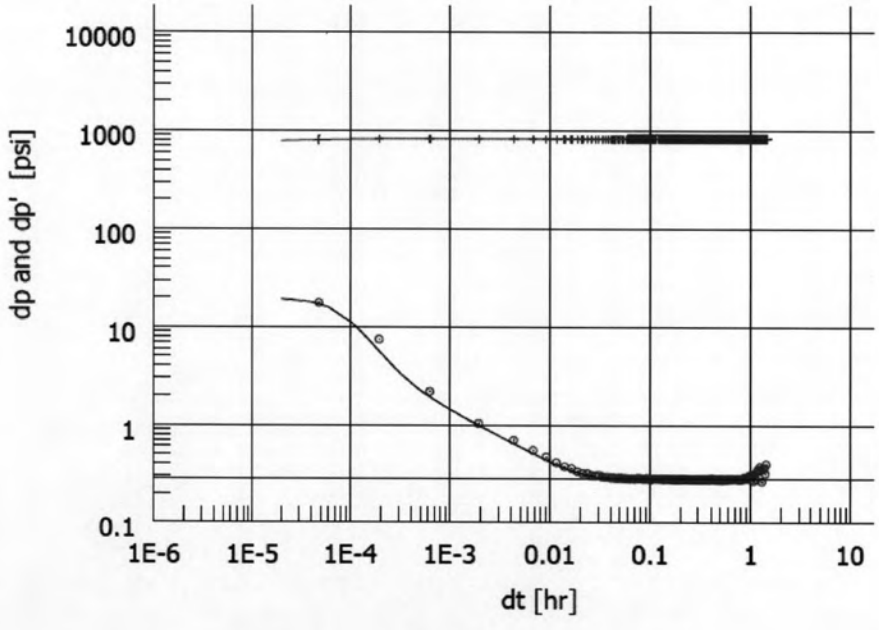

(d) Radius of stimulated zone = 3.35 ft.

Figure B6 : Regression plots for different radii of stimulated zone for case I(continued).

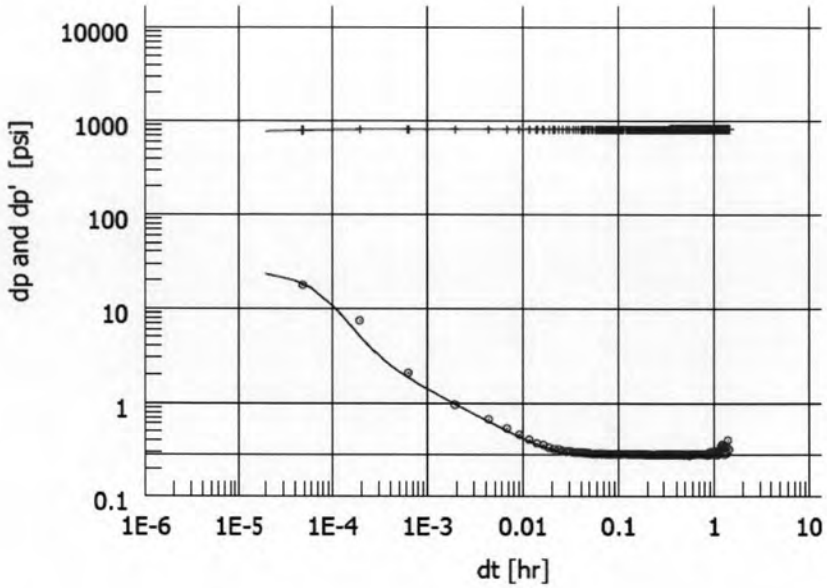

(e) Radius of stimulated zone = 4.56 ft.

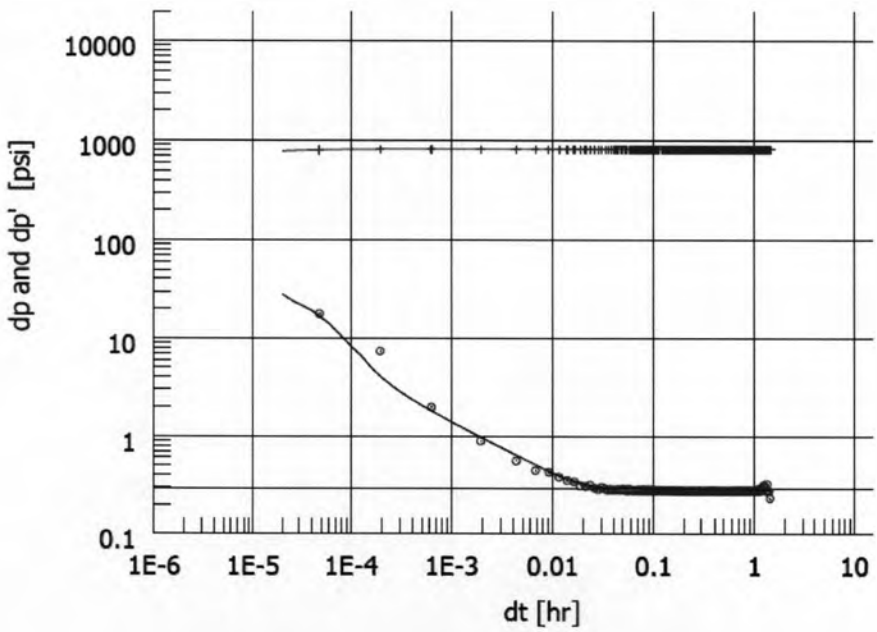

(f) Radius of stimulated zone = 6.19 ft.

Figure B6 : Regression plots for different radii of stimulated zone for case I (continued).

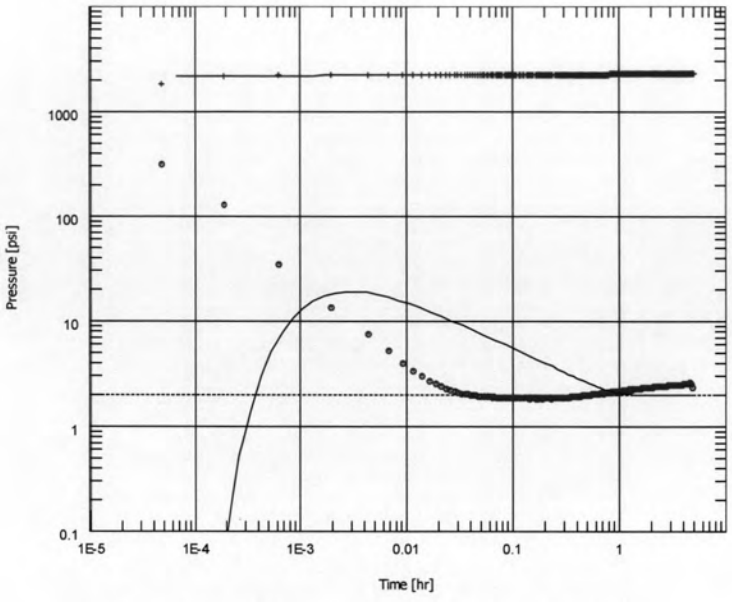

(a) Mobility ratio = 5

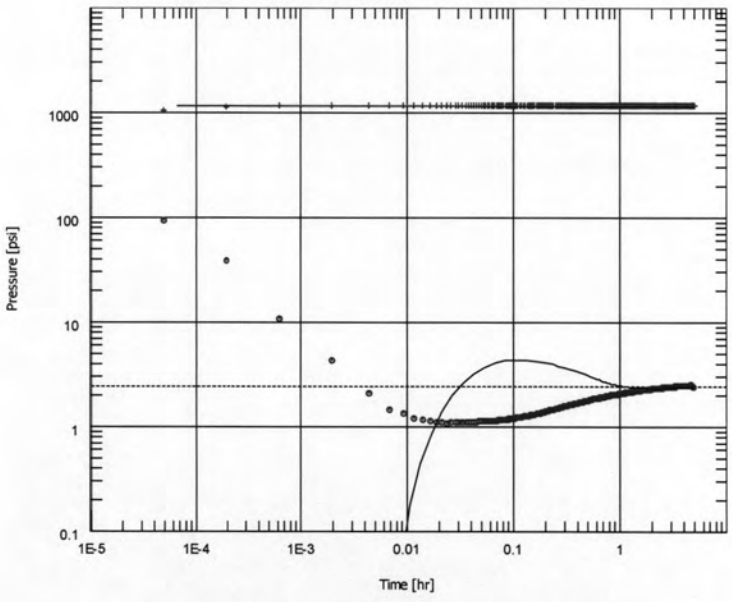

(b) Mobility ratio = 10

Figure B7 : Regression plots for different mobility ratios between stimulated zone and native reservoir for case II.

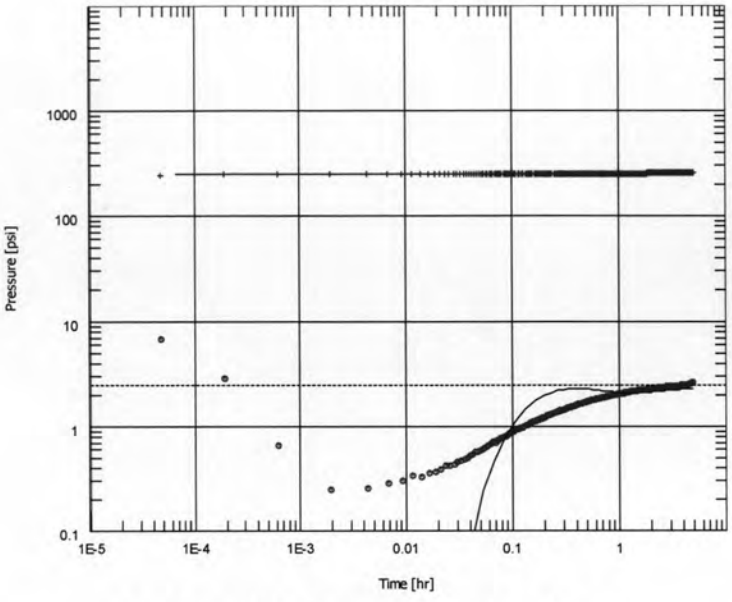

Log-Log plot: dp and dp' [psi] vs dt [hr]

(c) Mobility ratio = 50

Figure B7 : Regression plots for different mobility ratios between stimulated zone and native reservoir for case II (continued).

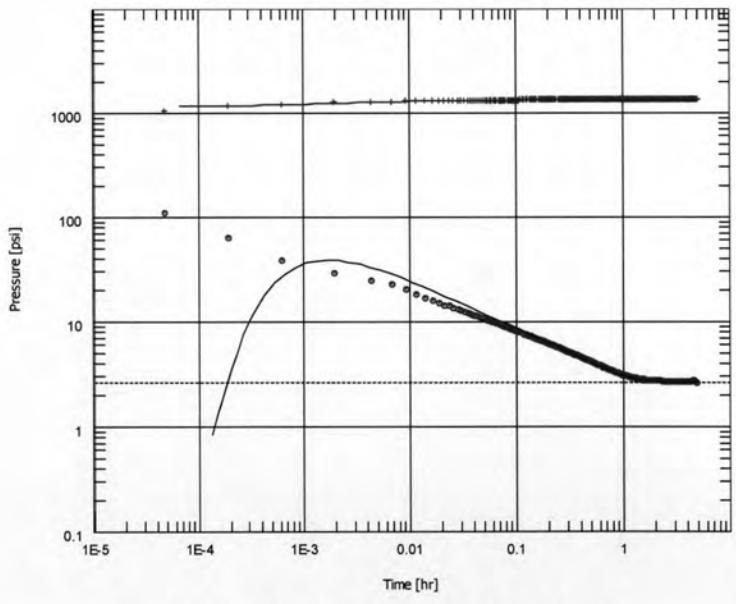

Log-Log plot: dp and dp' [psi] vs dt [hr]

(a) Radius of stimulated zone = 0.44 ft.

Figure B8 : Regression plots for different radii of stimulated zone for case II.

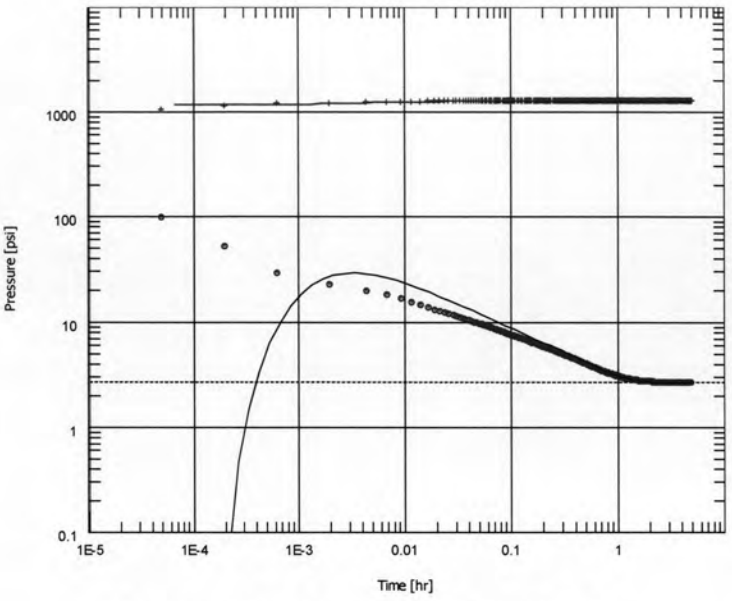

(b) Radius of stimulated zone = 0.64 ft.

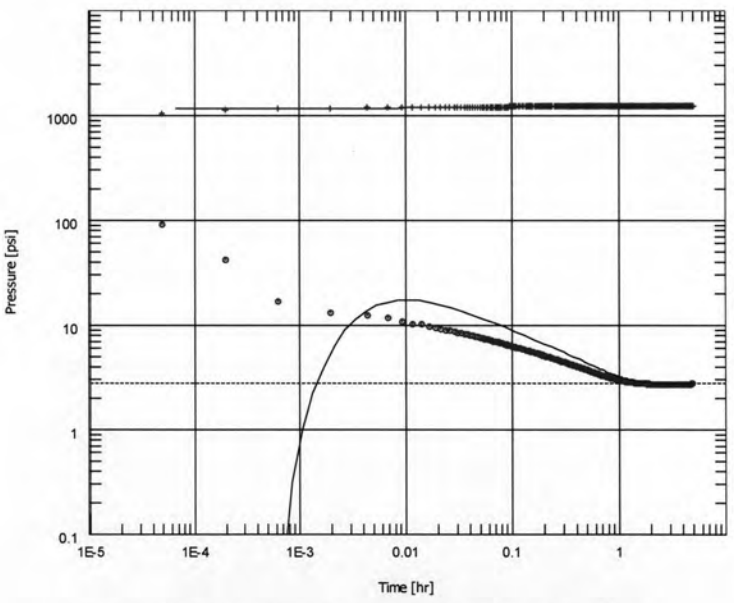

(c) Radius of stimulated zone = 1.28 ft.

Figure B8 : Regression plots for different radii of stimulated zone for case II (continued).

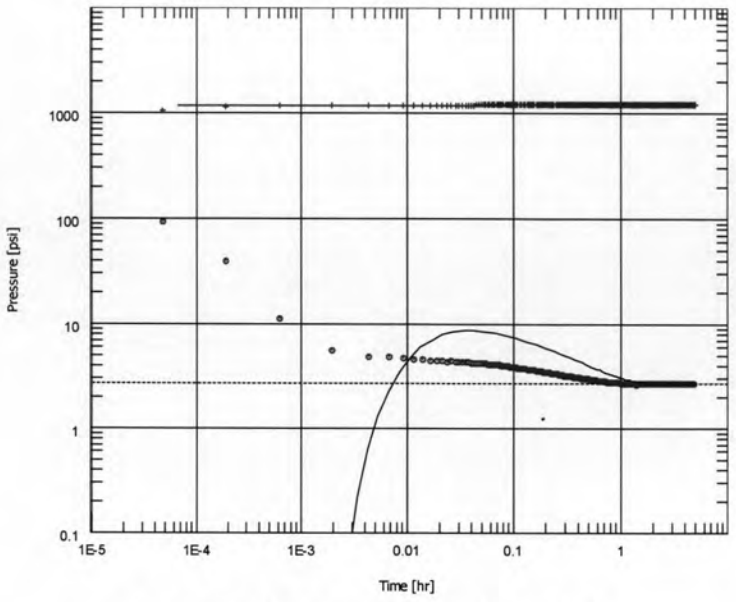

Log-Log plot: dp and dp' [psi] vs dt [hr]

(d) Radius of stimulated zone = 3.35 ft.

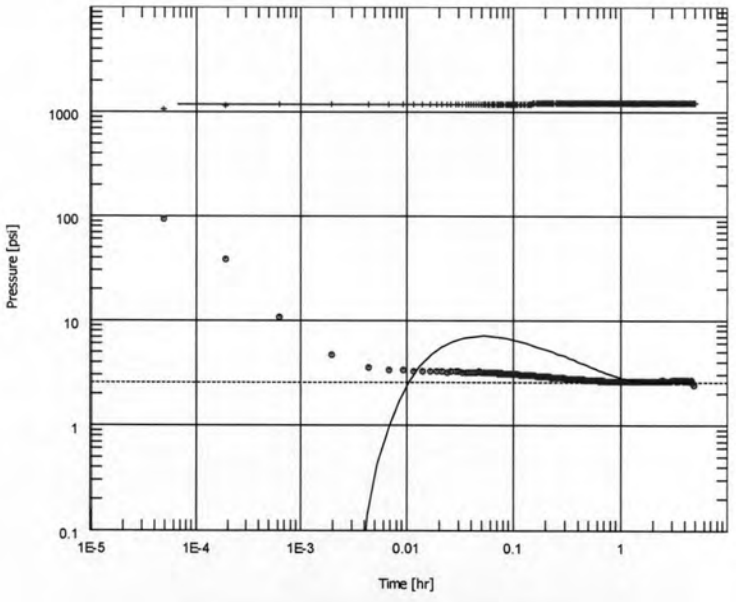

Log-Log plot: dp and dp' [psi] vs dt [hr]

(e) Radius of stimulated zone = 4.56 ft.

Figure B8 : Regression plots for different radii of stimulated zone for case II (continued).

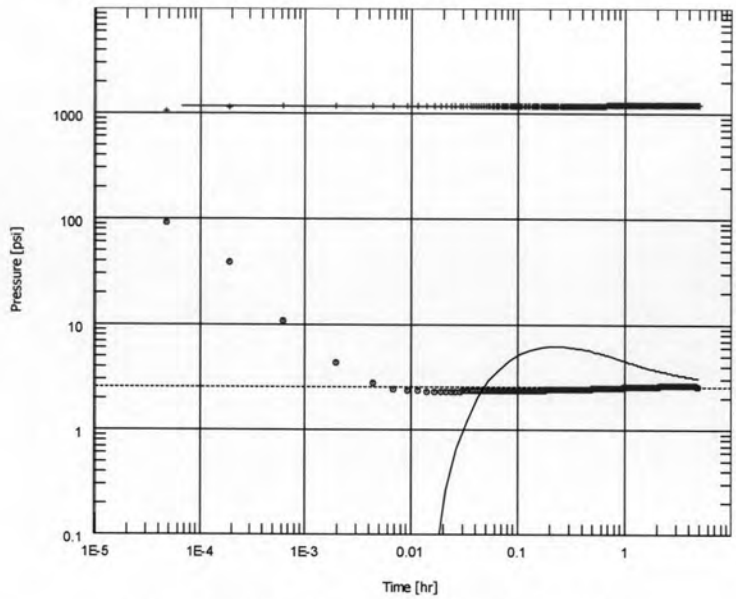

Log-Log plot: dp and dp' [psi] vs dt [hr]

(f) Radius of stimulated zone = 6.19 ft.

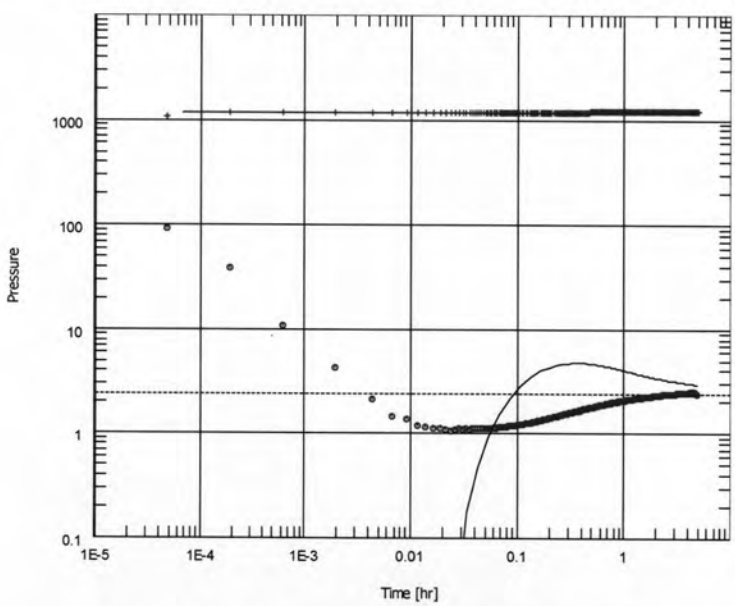

Log-Log plot: dp and dp' [psi] vs dt [hr]

(g) Radius of stimulated zone = 11.35 ft.

Figure B8 : Regression plots for different radii of stimulated zone for case II (continued).

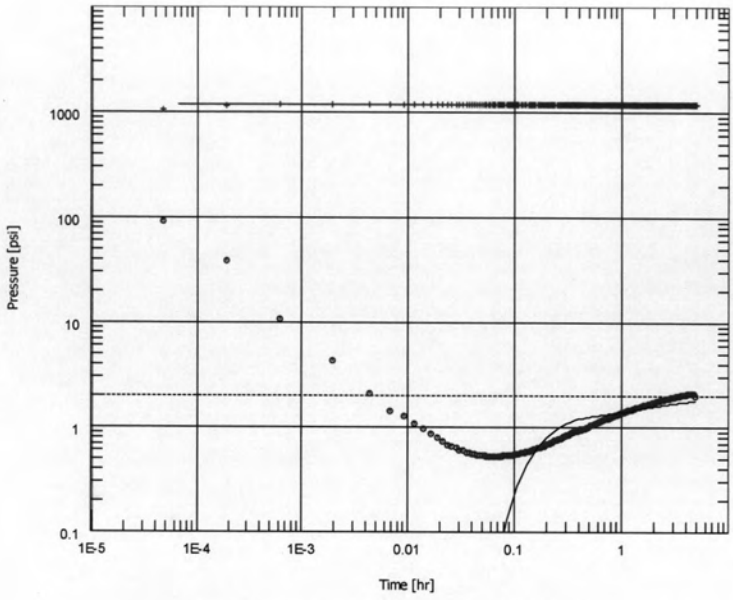

(h) Radius of stimulated zone = 20.71 ft.

Figure B8 : Regression plots for different radii of stimulated zone for case II (continued).

APPENDIX C

Wireline Formation Test and Interpretation Procedure

When the probe is set in the wellbore, a short test which is called a pretest, is conducted to measure the formation pressure. Formation fluid is withdrawn form the formation during the pretest. Both drawdown and buildup pressure data are acquired for each pretest.

Figure C1 shows a pressure versus time plot of a typical pretest. During the pretest, the formation fluid is withdrawn through the probe into the pretest chamber. This generates a localized flow in the formation that has a pattern essentially of spherical character. The drawdown pressure depends on the mobility, k/μ, of the flowing fluid which is usually mud filtrate in the invaded zone.

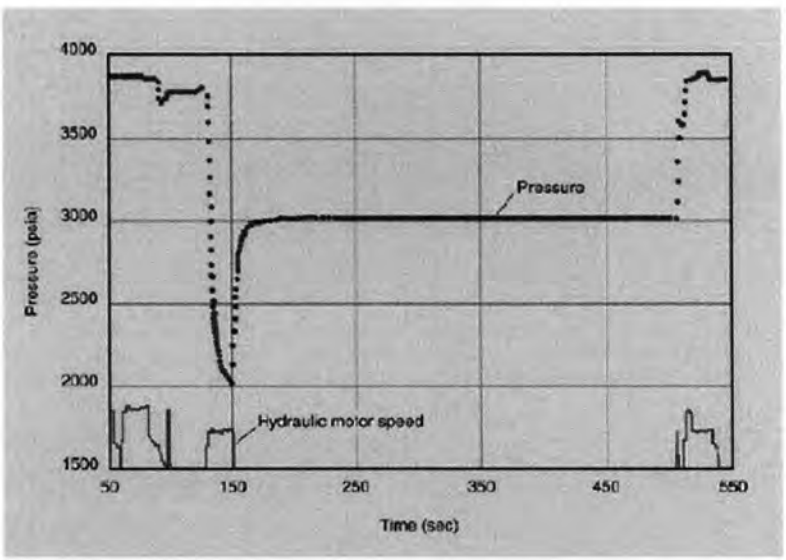

Figure C1 : Typical pressure versus time plot of a pretest.

At the end of the drawdown period, the pretest chamber is full and the buildup period starts. The pressure disturbance continues to advance in a pattern similar to the drawdown period because of fluid flowing from the undisturbed part of the formation toward the low-pressure area near the probe. The pressure measured at the probe rises

until it reaches the formation pressure. The time required for this buildup is essentially a function of the formation fluid mobility and the producing time.

During the buildup period, the pressure disturbance propagates spherically and continues in this manner until one impermeable barrier is reached. At this stage, the spherical flow pattern is altered and becomes hemispherical. Eventually, if a second vertical barrier is detected, the hemispherical propagation becomes radial.

The buildup data can be analyzed to obtain local estimations of mobilities of the undamaged zone. The first step consists of identifying the different flow regimes. These show up as characteristic patterns displayed by the pressure-derivative data. The pressure derivative is a popular transformation that indicates the rate of pressure change with respect to a selected time function.

Figure C2 shows constant-rate pressure-derivative curves for a pretest buildup. The dashed curve corresponds to the spherical time function and the solid curve to the radial time function. A time interval for which the derivative of the pressure with respect to the spherical time function has a flat trend should correspond to the time when the flow is spherical. During this interval, the derivative of the pressure with respect to the radial time function should have a slope of -½. Similarly, a time interval for which the derivative of the pressure with respect to the radial time function has a zero slope should correspond to the time when the flow is radial. During this interval, the derivative of the pressure with respect to the spherical time function should have a slope of +½.

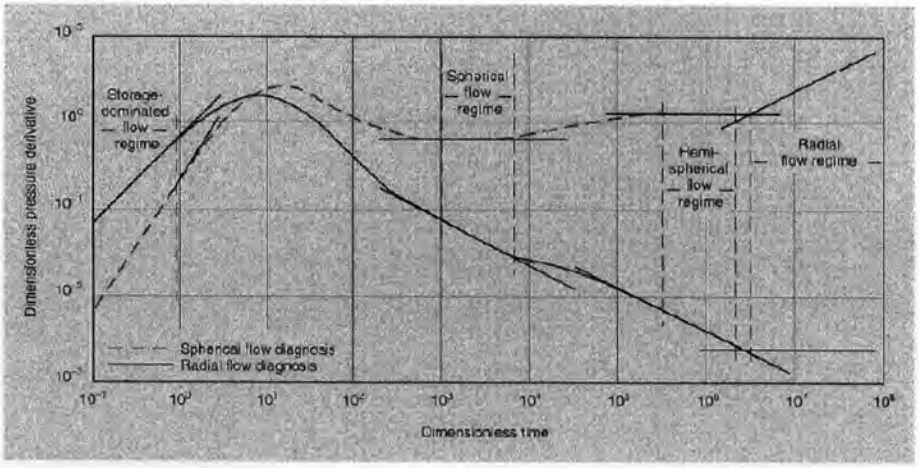

Figure C2 : Theoretical log-log plot of pressure derivative for a sink probe buildup.

Wireline Formation Testing Tools

Reservoir engineers use wireline formation testers to obtain pressure profiles, formation fluid samples and permeability indicators information that is crucial during exploration and development of oil and gas fields. Years of research and engineering efforts have been devoted to developing formation testers to help satisfy these objectives. The wireline formation tester was commercially used in 1955 in the Gulf of Mexico, primarily to recover one fluid sample and measure one formation pressure on each trip to the well. Later the Formation Interval Tester (FIT) was also introduced to the exploration activities. During the 1950s and 1960s, the logging cable conveyed wireline tester was mainly used to differentiate oil from gas in discovery wells. In the mid-1970s, Schlumberger introduced Repeat Formation Testers (RFT) replaced its predecessors FT or FIT, starting in the North Sea, which marked the beginning of a new era in wireline formation testing technology and application in the upstream oil industry. Shortly after, a variety of wireline testers were available on the market, satisfying the growing need of oil companies in their exploration and development projects. Beginning in the early 1990s, wireline tester technology took another huge leap forward. To provide solid answers to complex and varied reservoir questions, particularly fluid typing and sampling, Schlumberger designed a new modular tool, Modular Dynamics Formation Tester or MDT, marking a new revolution in wireline formation testing with much-enhanced features and capabilities. After that Baker-Atlas debuted its Reservoir Characterization Instrument RCI, and recently in 1999 Halliburton brought Reservoir Description Tool RDT to the marketplace.

Modern wireline formation testers are designed primarily to obtain pristine formation fluid samples soon after a well has been drilled. Fluids from the near wellbore region are pumped through a probe for an extended time interval until sensors in the tool determine that a minimal amount of filtrate contamination is present in the sample. Samples taken with this procedure are considered representative of PVT conditions when the sample contamination level is less than 10 percent. Additional measurements are recorded while sampling such as pressure vs. time and flow rate vs. time, while fluid sensors monitor the volume fractions of the fluids present in the flow lines. All of these measurements represent a comprehensive

pressure transient data set, that are dependent on a complex interaction of the wellbore overbalance, mud filtrate composition, mudcake formation properties and the in situ formation parameters. Three tools have been introduced over the past 10 years that can be classified as wireline formation testers, Schlumberger's MDT, Halliburton's RDT and Baker Hughe' RCI, lead the wireline testing services worldwide, all having multifunctional features for a broad span of reservoir evaluation applications, from pressures, fluid identification and sampling, to mini-drillstem testing and permeability evaluations. All these three testers are modular tools, each tool string has to be assembled by stacking all required modules before running into the well.

The tool can be arranged in a variety of configurations depending on testing needs. This study is emphasizing on MDT tool. The MDT string can be configured for the desired testing objectives. Formation pressure requirements are satisfied with the single-probe module, which can be placed virtually anywhere in the string. Permeability and permeability anisotropy measurements can be addressed with the multiprobe module, two single-modules run in tandem, or the dual packer module. Pressure-volume-temperature (PVT) quality fluid sampling requirements can be satisfied by the combination of sample chamber modules, dump chambers, multisample modules, OFA Optical Fluid Analyzer and pumpout module (Figure C3). The following section includes a brief description of the available modules.

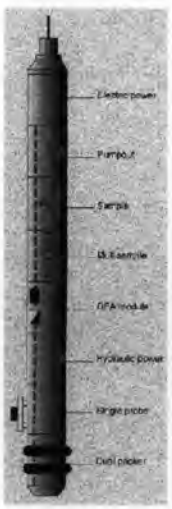

Figure C3 : MDT tool with all modules.

Standard MDT Tool

Figure C4 shows a schematic of the MDT tool with the single-probe module. The tool is designed to take several pressure measurements and fluid samples during one trip in the well. This configuration, which extends the capabilities of existing single-probe testers, provides a basic tool to which additional modules and therefore capabilities can be added. Advantages over existing tools include flowline temperature and flowline fluid resistivity determinations, collection of several fluid samples per trip, standard operations in a larger range of hole sizes, extended pressure accuracy and dynamic response, and surface controlled pretest rate, volume and sampling pressure. The tool is usually combined with a gamma ray device for depth control and an Auxiliary Measurement Sonde (AMS) tool for tension monitoring.

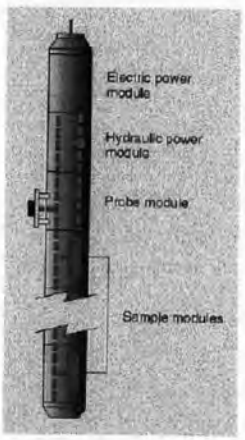

Figure C4 : Standard MDT tool configuration for single-probe tools.

Normally the top section of each module houses the electronics and the bottom section contains the hydraulics and valves. The main hydraulic communication takes place along a hydraulic bus that runs through the hydraulic power module and the single-probe module. Any module needing hydraulic power must be connected immediately next to the hydraulic power module. This also means that modules that do not have a hydraulic bus cannot be connected between modules using the hydraulic bus. For example, a sample chamber cannot be placed between a hydraulic power module and a single-probe module.

Electric power module

The electric power module converts AC power from the surface to provide tool electrical DC power along a common electrical bus running through all modules. The electric power module is used in every MDT configuration and always at the top of the tool string.

Hydraulic power module

The hydraulic power module contains an electric motor and a hydraulic pump and is the basic hydraulic power source, delivering power by way of a hydraulic bus. Its 50-V DC electric motor drives a fixed- displacement hydraulic pump (i.e., constant volume per revolution). A fixed-displacement pump allows the estimation of the volume of oil pumped by counting the motor revolutions, thus allowing the determination of pretest volume in the probe.

The module also has a hydraulic accumulator, which stores energy with the aid of a large spring and piston. If tool power is lost, this stored energy is connected to the hydraulic bus to automatically close the probe. In addition, a differential pressure gauge monitors pump output pressure. Through-flowline and electrical connections allow running the hydraulic power module anywhere in the tool string below the electric power module.

Single-probe module

Connected directly to the hydraulic power module, the single-probe module contains a probe assembly with packer and telescoping backup pistons and connects the tool flowline to the reservoir. It also houses the strain and quartz gauges and fluid resistivity and temperature sensors and provides pretest functions. The single-probe module can be placed anywhere in the string, but it must be directly connected to the hydraulic power module.

The probe extends against the borehole wall to provide a sealed fluid path from the reservoir to the flowline. The pretest is used to ensure a good hydraulic seal,

obtain accurate formation pressure recordings and determine permeability. The module has one pretest chamber with a maximum volume of 20 cm^3. The MAXIS 500* service unit controls the sampling pressure, pretest flow rate and volume from the surface. This allows the engineer to select optimal values for the various formation characteristics that can occur during a pressure measurements sequence.

New features include a flowline resistivity sensor, temperature sensor and isolation valve. The resistivity measurement helps to discriminate filtrate from water-base muds and formation fluids. It is also useful when taking formation water samples in wells drilled with oil-base mud. The isolation valve minimizes the effects of flowline fluid volume on pressure transients by reducing the flowline volume during a pretest. This is needed because the complete flowline bus in a long string has a significant volume and can distort the pressure test profile through the "storage effect" which is caused by the finite compressibility of the flowline fluid. The isolation valve also serves to isolate the probe in the case when more than one probe is present in the string.

Pressure measurement

For measuring pressure, what is needed is a high accuracy, high resolution gauge with fast dynamic response to quickly recover from the various pressure shocks that it experiences during the job.

The single-probe module is equipped with two optional sensors for measuring the flowline pressure which are strain and quartz gauges.

- Strain gauge

The strain gauge used in the single-probe module is a bonded-wire strain gauge. The bonded-wire sensor consists of a tube with a strain wire wrapped around it. The applied pressure on the tube causes the strain wire to stretch, thereby inducing a change in electrical resistance.

- CQG Crystal Quartz Gauge

The most accurate pressure sensors use quartz crystals. A correctly cut section of quartz has a natural, or resonant, frequency of vibration like a tuning fork. As the quartz vibrates, there is a detectable sinusoidal variation in electrical charge on its surface. Pressure induced stress applied to the crystal causes the sine wave frequency to vary in a highly precise manner.

Sample chambers

The standard sample chambers are available with volumes of 1, 2 ¾ and 6 gal. Each chamber has an electromechanically actuated throttle (seal) valve, which is controlled from the surface and directs sampled fluid to the selected chamber in any order. The valve can operate in one of two modes. In seal mode, the valve can be either fully open or fully closed. In throttle mode, the valve operates as a variable orifice that automatically opens and closes to maintain the flowing pressure constant. The throttle valve is a dynamic valve, constantly adjusted to maintain a specified flowline sampling pressure within an error band. In addition, the sample chamber has a drain valve for connecting the sample drainage equipment and a transport valve for sealing the sample in the module.

Optional modules

There are six available optional MDT modules can be added to the basic tool.

1) **Dual probe module** – The dual probe consists of two probes (sink and horizontal probes) mounted diametrically opposite to each other. The sink, or flowing, probe is connected to the flowline. The horizontal probe is not connected to the flowline bus and is used exclusively as a monitor probe. The dual probe module does not operate in stand-alone mode but functions as a slave to the single-probe module and receives hydraulic power from the hydraulic power module via the single-probe module. The module's construction is such that the electronics section is at the bottom and the sonde

section is at the top. Therefore, the probes are placed 2.3 ft apart when the dual probe is connected to the single-probe module.

2) **Multiprobe system** – The probe at the single-probe module is called the vertical probe. With this configuration, the vertical and horizontal mobilities can be determined by performing a localized interference test (Figure C5). Under normal operations, the sink probe withdraws fluid from the formation at a prescribed rate, while the vertical and horizontal probes monitor the pressure response.

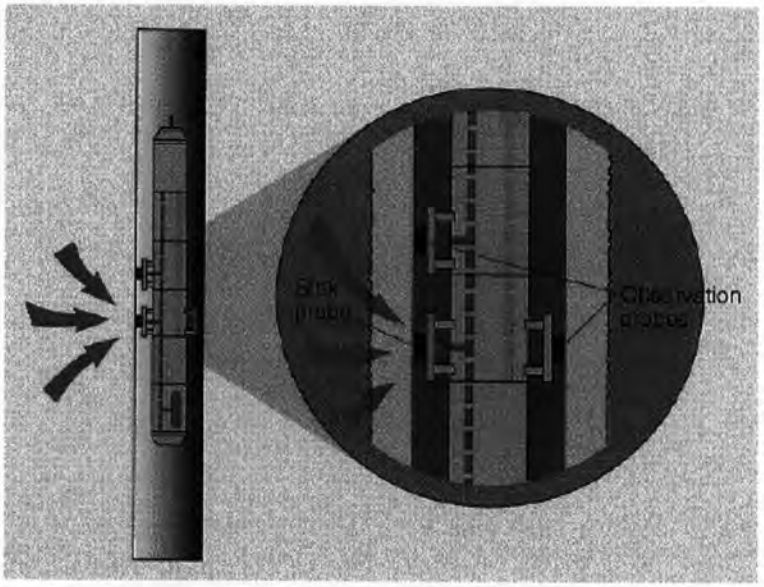

Figure C5 : Location of sink probe and observation probes.

3) **Flow control module** – This module can pulse the formation to a greater depth and control the pulse for greater accuracy when determining vertical permeability. The module provides the ability to control and measure the sampling flow rate. Operational modes for the flow control module include constant flow rate, constant pressure and ramped flow rate or pressure.

4) **Dual packer module** – provides two inflatable packer elements to isolate a borehole interval for testing and/or sampling. Spacing between the packer elements varies with hole size, but the minimum distance is about 3 ft. The

entire borehole wall is open to the formation, so the fluid flow area is several thousand times larger than with conventional probes. The dual packer module can be used as an alternative to conventional probes.

5) **Pumpout module** – it pumps fluid directly from the formation into the mud column. The pumpout module eliminates the volume limitation on the amount of fluid dumped. The module can also be used to pump fluid from the borehole into the flowline to inflate the packers of the dual packer module. The module has the capability to pump within the flowline. An additional advantage of the pumpout device is the ability to limit the drawdown pressure applied to the formation, which greatly reduces seal failures.

6) **OFA module** – some conditions, and particularly wells drilled with OBM, may require the OFA module. This module, run immediately below the probe module as shown in Figure C3, uses optical analysis techniques to identify the fluid in the flowline. The flowline passes through two independent optical sensors (Figure C6). In one cell, absorption spectroscopy is used to detect and analyze liquid, while in the other cell, a special type of optical reflection measurement detects gas.

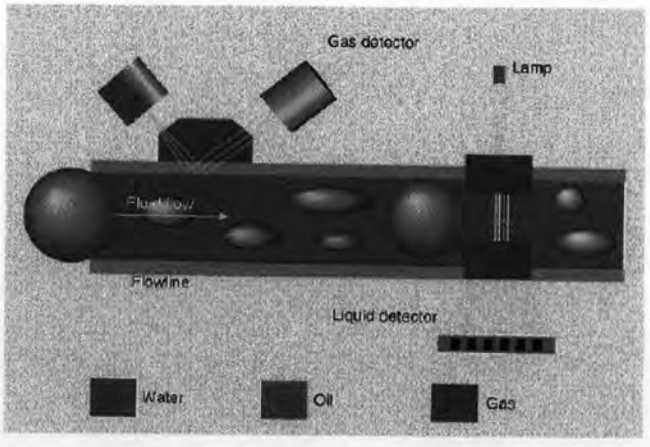

Figure C6 : The OFA module with its two sensor systems.

7) **Multisample module** – this module contains six sample chambers mounted in a single carrier. Each sample cylinder collects a 450 cm^3 sample suitable for full PVT analysis. Surface-controlled valves open and close specific sample bottles as required. This makes it possible to take multiple samples bottles at various well depths.

VITAE

Naruewan Tantipalanonta was born on January 3, 1983 in Bangkok, Thailand. She received her B.Eng. in Chemical Engineering from the Faculty of Engineering, Chulalongkorn University in 2005. After graduating, she continues her studies in the Master of Petroleum Engineering program at the Department of Mining and Petroleum Engineering, Faculty of Engineering, Chulalongkorn University.